ImmunoTargets and Therapy

Dovepress
Taylor & Francis Group

Open Access Full Text Article

ORIGINAL RESEARCH

Lysyl Oxidase-Like 1 (LOXL1) Up-Regulation in Chondrocytes Promotes M1 Macrophage Activation in Osteoarthritis via NF-κB and STAT3 Signaling

Yuyun Jiang[1,*], Shang Wang[2,*], Wei Zhu[1,3], Xi Liu[1], Yanwei Yang[1], Liyue Huo[1], Jixian Ye[1], Yongbin Ma[1,4], Yuepeng Zhou[1], Zhe Yang[1], Jiahui Mao[1], Xuefeng Wang[1,5]

[1]Department of Central Laboratory, The Affiliated Hospital of Jiangsu University, Zhenjiang, 212001, People's Republic of China; [2]Tzu Chi International College of Traditional Chinese Medicine, Vancouver, BC, Canada; [3]Department of Sports Medicine, The Affiliated Hospital of Jiangsu University, Zhenjiang, 212001, People's Republic of China; [4]Department of Central Laboratory, Jintan Hospital, Jiangsu University, Jintan, 213200, People's Republic of China; [5]Department of Nuclear Medicine, Institute of Digestive Diseases, and Institute of Endocrinology, The Affiliated Hospital of Jiangsu University, Zhenjiang, 212001, People's Republic of China

*These authors contributed equally to this work

Correspondence: Xuefeng Wang, Email xuefengwang@ujs.edu.cn

Purpose: Osteoarthritis (OA) constitutes a widespread degenerative joint disease predominantly affecting the elderly, leading to disability. There is still a lack of biomarkers for OA, so it cannot be intervened in time.

Methods: OA biomarkers were identified from human cartilage datasets using LASSO and SVM-RFE, followed by ROC analysis. LOXL1 was prioritized for further research due to its high expression in OA cartilage and robust predictive performance. Anterior cruciate ligament transection (ACLT) surgery-induced OA rats were used to explore the correlation between LOXL1 and inflammatory factors and macrophages. Macrophage markers and cytokine secretion were detected from macrophages treated with LOXL1, or co-cultured with chondrocytes after LOXL1 siRNA silencing.

Results: Five hub biomarkers with OA-specific expression were identified. Elevated LOXL1 correlated with IL-6 and IL-8 in patients and increased M1 macrophages in OA rats. LOXL1-stimulated macrophages upregulated CD86 and inflammatory cytokines. Silencing LOXL1 in chondrocytes reduced CD86, inflammatory cytokines, and NF-κB p65 and p-STAT3 expression in co-cultured macrophages, mitigating MMP13 and chondrocyte apoptosis. STAT3 and NF-κB signal inhibition reduces p-STAT3, p-p65, CD86, IL-6 and IL-1β expression in LOXL1-stimulated macrophages.

Conclusion: This study underscores the pivotal role of LOXL1 in activating M1 macrophages through NF-κB and STAT3 signaling, thereby promoting pro-inflammatory cytokine secretion and contributing to OA pathogenesis. LOXL1 holds promise as a potential marker for early diagnosis of OA inflammation and as a novel therapeutic target.

Keywords: lysyl oxidase-like 1, LOXL1, chondrocytes, macrophage activation, up-regulation, osteoarthritis

Introduction

Osteoarthritis (OA) remains a predominant degenerative joint ailment causing disability among the elderly. Current estimates indicate that 10% of the global population suffers from this condition,[1] with nearly half of those aged 60 and above experiencing OA, highlighting its significant contribution to disability.[2] Consequently, OA imposes a considerable economic burden on patients and public health systems worldwide, presenting a formidable challenge for aging societies.[3] Conventional imaging techniques continue to be the "gold standard" for clinical OA diagnosis. However, assessing joint space width through plain radiography often requires ongoing evaluation over 1 to 3 years. While magnetic resonance imaging (MRI) offers enhanced sensitivity in detecting cartilage, bone, synovial effusion, and

Received: 17 December 2024
Accepted: 16 March 2025
Published: 24 March 2025

ligament changes, its widespread use is limited by high costs.[4] The lack of reliable diagnostic methods for detecting and monitoring joint pathological changes poses a significant barrier to halting the clinical progression of OA.

OA manifests as the progressive degeneration of cartilage and ligaments, coupled with synovial inflammation. Chondrocytes, the primary cellular components of articular cartilage, are critically implicated in regulating cartilage homeostasis.[1] Despite advancements in understanding OA pathogenesis, the precise mechanisms by which chondrocytes promote joint catabolic activity remain incompletely understood. Notably, chondrocytes interact with synovial immune cells, initiating synovial inflammation in the early stages of OA.[5] Long-term inflammation results in cartilage loss and progressive joint degeneration.[6,7] Within the synovium, macrophages represent the predominant immune cell population, with activated synovial macrophages releasing pro-inflammatory cytokines like IL-1β, TNF-α, and IL-6, which in turn stimulate chondrocytes to produce matrix metalloproteinases and aggrecanases such as MMP-3, MMP-13, ADAMTS-4, and ADAMTS-5. These enzymes lead to the degradation of extracellular matrix (ECM) components, including type II collagen (COL II) and aggrecan (ACAN).[8,9] Degraded cartilage also releases inflammatory cytokines such as IL-6, IL-8, IL-1β, and TNF-α, creating an inflammatory environment within the joints.[10] Given the pivotal role of inflammation in initiating OA, there is significant interest in identifying specific biomarkers that reflect macrophage activation and inflammatory responses. Additionally, new insights into the interactions between chondrocytes and synovial macrophages provide novel perspectives for understanding OA pathogenesis comprehensively.

This study, utilizing the GEO database within the R language and incorporating three microarray datasets (GSE178557, GSE183531, and GSE169077) alongside one transcriptome RNA-seq dataset (GSE114007), elucidates the close association between the chondrocyte-expressed LOXL1 gene and OA through bioinformatics and machine learning. The Lysyl oxidase-like 1 (LOXL1) protein, encoded by the LOXL1 gene and a member of the lysyl oxidase family, plays a critical role in preserving ECM-rich tissues.[11] LOXL1 has been implicated in the pathogenesis of diverse maladies such as glaucoma,[12] intrahepatic cholangiocarcinoma,[13] and glioma.[14] Our study revealed heightened expression of the LOXL1 gene and protein in patients with OA, correlating positively with cytokines IL-6 and IL-8. Additionally, augmented expression of LOXL1 and IL-6 was observed in the cartilage of OA rats, along with increased $iNOS^+$ M1 macrophage expression in the synovium, with LOXL1 showing positive correlations with IL-6 and iNOS. Stimulation of macrophages with LOXL1 protein resulted in elevated CD86 expression and cytokine secretion, indicating that LOXL1 is a potential biomarker of OA inflammation. Moreover, inhibiting chondrocyte LOXL1 expression may represent a novel strategy for OA therapy.

Material and Methods

Data Acquisition and Processing

The GSE178557, GSE183531, GSE169077, and GSE114007 datasets were sourced from the NCBI GEO public database (http://www.ncbi.nlm.nih.gov/geo). GSE178557 includes 8 cartilage samples (n = 4 for the OA group, n = 4 for the control group). GSE183531 includes 5 cartilage samples (n = 5 for the OA group). GSE169077 includes 11 cartilage samples (n = 6 for the OA group and n = 5 for the control group). GSE114007 includes 38 cartilage samples (n = 20 for the OA group, n = 18 for the control group). Datasets of the same sequencing type were analyzed collectively. The three microarray datasets—GSE178557, GSE183531, and GSE169077—were merged to form the training set, with batch effects adjusted using the combat function from the "SVA" package in R. The RNA-seq dataset, GSE114007, served as the verification set. All datasets underwent standardized data preprocessing.

Identification of Differentially Expressed Genes (DEGs)

Differentially expressed genes (DEGs) were identified from the GSE178557, GSE183531, and GSE169077 datasets using the "limma" package for variance analysis, applying a filter condition of an adjusted p-value < 0.05 and log fold change > 1. A heatmap of DEGs was generated with the "ggplot2" package. Additionally, the RNA-seq dataset GSE114007 served as an independent validation set, where batch effects were removed and differential analysis was conducted using the "DESeq2" package.

Candidate Diagnosis Biomarker Selection

A comprehensive biomarker screening approach was employed, utilizing the Least Absolute Shrinkage and Selection Operator (LASSO) logistic regression model and the Support Vector Machine Recursive Feature Elimination (SVM-RFE) algorithm to identify OA-related biomarkers. LASSO, a regression analysis method enhanced by regularization, effectively improves predictive accuracy. The "glmnet" package in R facilitated this analysis, pinpointing genes significantly contributing to the discriminatory power between OA and healthy samples. Support vector machine (SVM), a supervised machine learning technology extensively used for classification and regression analysis, was applied with Recursive Feature Elimination (RFE) to select the optimal genes from the metadata cohort, thereby preventing overfitting. SVM-RFE identified the most discriminative gene set, implemented via the R packages "e1071" "kernlab" and "caret." Overlapping genes were then screened for further analysis.

Diagnostic Value of Feature Biomarkers in OA

The diagnostic ability of biomarkers was assessed by quantifying their sensitivity and specificity through receiver operating characteristic (ROC) curve analysis and measuring the area under the curve (AUC). The accuracy, sensitivity, and specificity of these biomarkers were determined in the training set using the R package "pROC" and subsequently validated in the verification set.

Clinical Specimens

Blood samples were collected from newly diagnosed, untreated patients with OA and a healthy cohort aged 50–85 years, without osteoarthritis or rheumatoid arthritis. Exclusion criteria included post-medication follow-up, malignancies, severe infections, endocrine or immune disorders, organ dysfunction, and psychiatric illnesses, to prevent interference with natural cytokine levels. Written informed consent for blood sample usage was obtained from all participants. Human blood sample procedure was in accordance with the ethical standards laid down in the 1964 Declaration of Helsinki and all subsequent revision. The Ethics Committee of the Affiliated Hospital of Jiangsu University approved the study (KY2023K1109).

Quantitative Real-Time PCR (qRT-PCR)

Total RNA was extracted from blood samples of patients with OA and healthy individuals using the RNAeasy™ Blood RNA Isolation Kit with Spin Column (Beyotime, Shanghai, China), and from cells using TRIZOL reagent (Invitrogen, California, USA) according to the manufacturer's instructions. Reverse transcription reactions were performed following the HiScript II Q RT SuperMix for qPCR (Vazyme, Nanjing, China) protocol, followed by real-time fluorescence quantitative PCR (qPCR) using ChamQ Universal SYBR qPCR Master Mix (Vazyme, Nanjing, China). All data were normalized to GAPDH expression levels. The primers used were: LOXL1 (Homo sapiens): forward (5′-TGTACCGGCCCAACCAGAAC-3′) and reverse (5′-CCGCACATCGTAGTCGGT-3′); GAPDH (Homo sapiens): forward (5′-GTCTCCTCTGACTTCAACAGCG-3′) and reverse (5′-ACCACCCTGTTGCTGTAGCCAA-3′); LOXL1 (Mus musculus): forward (5′-ATGTGCAGCCTGGGAACTAC-3′) and reverse (5′-GCGACCTGTGTAGTGGATGT-3′); GAPDH (Mus musculus): forward (5′-CATCACTGCCACCCAGAAGACTG-3′) and reverse (5′-ATGCCAGTGAGCTTCCCGTTCAG-3′).

Enzyme-Linked Immunosorbent Assay (ELISA) and Measurement of Cytokine Levels

Quantification of LOXL1 in serum and cell culture supernatants was conducted using an ELISA kit (Cusabio, Wuhan, China), following the manufacturer's instructions. Cytokine levels in serum and cell culture supernatants were quantified using a twelve-cytokine detection kit (Biopredia, Taizhou, China) through multiplex flow cytometry luminescence, also following the manufacturer's instructions.

Experimental Animals

Female Sprague-Dawley (SD) rats (6–8 weeks old, weighing approximately 250–300 grams) were housed under standard conditions (22±1°C, 65–70% humidity). The rats were randomly assigned to two groups: sham surgery and anterior cruciate ligament transection (ACLT) surgery. After anesthesia with 2% pentobarbital sodium, the right knee joints were surgically prepared in a sterile manner. The anterior cruciate ligament was transected using a scalpel without damaging surrounding structures. The incision was sutured to ensure proper healing. Prophylactic antibiotic treatment (30,000 units of penicillin) was administered daily for 3 days post-surgery. After 9 weeks, the right knee cartilage and surrounding synovial tissue were collected and fixed with 4% paraformaldehyde for further analysis. All animals were provided humane care, and were conducted in accordance with the Guidelines for the Protection and Use of Experimental Animals and the Measures for the Administration of Animal Use at Jiangsu University. The experimental procedures received approval from the Institutional Animal Care and Use Committee (IACUC) of Jiangsu University (Permit Number: UJS-IACUC-AP-2023022005).

Immunohistochemistry (IHC) and Immunofluorescence (IF) Staining in vivo

Rat cartilage tissues were fixed in formaldehyde and decalcified with EDTA solution for 35 days. Subsequently, the tissues were dehydrated, embedded in paraffin, sectioned, and subjected to antigen retrieval. Endogenous peroxidase and serum were blocked before overnight incubation with primary antibodies against LOXL1 (Boster, Wuhan, China; diluted 1:50), IL-6 (Servicebio, Wuhan, China; diluted 1:50), and IL-10 (Servicebio, Wuhan, China; diluted 1:50). This was followed by incubation with secondary antibodies (Servicebio, Wuhan, China; diluted 1:50). DAB staining and hematoxylin counterstaining were performed to visualize cell nuclei, and microscopic examination was conducted.

For immunofluorescence staining, samples underwent similar initial processing as in immunohistochemical analysis. A mixture of primary antibodies against iNOS (Servicebio, Wuhan, China; diluted 1:50) and CD11b (Servicebio, Wuhan, China; diluted 1:50), as well as Arg1 (Servicebio, Wuhan, China; diluted 1:50) and CD11b (Servicebio, Wuhan, China; diluted 1:50), was added. Following overnight incubation, corresponding secondary antibodies (Servicebio, Wuhan, China; diluted 1:100) were applied, and DAPI was used to counterstain cell nuclei. Images were captured using a laser confocal microscope.

Flow Cytometry

Cells were stained with fluorophore-conjugated monoclonal antibodies following established protocols. Cultured cells were washed with PBS, centrifuged, and the supernatant discarded. The cells were then resuspended in a staining buffer and stained with anti-CD86 (BD Biosciences, San Diego, USA; 5μL / Test) for 30 minutes at 4°C in the dark. After two washes, the cells were suspended in a staining buffer. Using the same method, cells were collected, fixed, permeabilized, and stained with anti-CD206 (Biolegend, San Diego, USA; 5μL / Test), followed by incubation at 4°C in the dark for 60 minutes. After two additional washes, the cells were resuspended in staining buffer and analyzed using flow cytometry. Chondrocyte apoptosis was assessed with the ANNEXIN V-FITC/PI apoptosis detection kit (Solarbio, Beijing, China) according to the manufacturer's instructions.

Cell Culture and Small-Interfering RNA Transfection

ATDC5, RAW264.7, and THP-1 cells were obtained from Shanghai Zhong Qiao Xin Zhou Biotechnology (Shanghai, China). ATDC5 cells were cultured in Dulbecco's Modified Eagle Medium/Nutrient Mixture F-12 (DMEM/F-12) supplemented with 1% Penicillin-Streptomycin Solution and 10% Fetal Bovine Serum (FBS). RAW264.7 cells were cultured in Dulbecco's Modified Eagle Medium (DMEM) supplemented with 1% Penicillin-Streptomycin Solution and 10% FBS. THP-1 cells were maintained in RPMI-1640 medium enriched with 1% Penicillin-Streptomycin Solution, 0.05 mm β-Mercaptoethanol, and 10% FBS. Differentiation of THP-1 cells into macrophages was achieved by adjusting the cell density to 1×10^6 cells/mL, adding 100 ng/mL of Phorbol-12-myristate-13-acetate (PMA), and incubating at 37°C with 5% CO2 for 24 hours until adherence. Macrophages were treated with recombinant Human LOXL1 protein (Cusabio, Wuhan, China), NF-κB inhibitor SC75741 (Abmole, Shanghai, China), STAT3 inhibitor Stattic (APExBIO, Houston, USA), or the above inhibitors combined with LOXL1 stimulation for 48 hours.

Si-LOXL1 was procured from Nanjing Zebrafish Biotech (Nanjing, China). ATDC5 cells were seeded in 6-well plates and transfected after 24 hours of incubation. Using Lipo6000 transfection reagent (Beyotime, Shanghai, China), negative control (NC-siRNA), LOXL1-siRNA1, and LOXL1-siRNA2 were introduced into the chondrocytes. Cellular RNA and proteins were collected 48 hours post-transfection for analysis of transfection efficiency.

Co-Culture

Following the established transfection protocol, LOXL1-siCTRL (NC-siRNA), LOXL1-siRNA1, and LOXL1-siRNA2 were transfected into chondrocytes and cultured for 48 hours. Utilizing a Transwell system, ATDC5 cells treated as previously described were placed in the lower chamber and stimulated with IL-1β (10 ng/mL), while THP-1-induced macrophages were situated in the upper chamber for co-culture over 72 hours, or RAW264.7 cells were seeded in the upper chamber for 48 hours. Subsequently, THP-1-induced macrophages were collected for flow cytometry analysis, and their supernatant was utilized for ELISA to measure LOXL1 secretion.

Following co-culture, RAW264.7 cells were harvested for Western blot analysis. For the rescue experiments, RAW264.7 cells co-cultured with ATDC5 cells transfected with LOXL1-siRNA1 were stimulated with 8 μg/mL recombinant mouse LOXL1 protein (Cusabio, Wuhan, China) for 24 hours. Subsequently, RAW264.7 cells from the upper chamber were harvested for Western blot analysis.

Western Blotting

Cell samples were lysed in lysis buffer (Beyotime, Shanghai, China), and denatured proteins were separated via sodium dodecyl sulfate-polyacrylamide gel electrophoresis before being transferred onto polyvinylidene difluoride membranes (Millipore, Billerica, USA). These membranes were blocked with 5% skim milk and incubated overnight at 4°C with primary antibodies: anti-LOXL1 (Boster, Wuhan, China; diluted 1:500), anti-MMP13 (Proteintech, Wuhan, China; diluted 1:1000), anti-p-STAT3 (Affinity, Jiangsu, China; diluted 1:500), anti-STAT3 (Proteintech, Wuhan, China; diluted 1:2000), anti-p-p65 (Proteintech, Wuhan, China; diluted 1:2000), anti-p65 (Santa Cruz, California, USA; diluted 1:200), anti-CD86 (Proteintech, Wuhan, China; diluted 1:1000), anti-Arg1 (Proteintech, Wuhan, China; diluted 1:5000), anti-human-IL-6 (Proteintech, Wuhan, China; diluted 1:500), anti-IL-1β (Proteintech, Wuhan, China; diluted 1:1000), anti-TNF-α (Affinity, Jiangsu, China; diluted 1:500), anti-GAPDH (Proteintech, Wuhan, China; diluted 1:10,000), anti-IL-10 (Servicebio, Wuhan, China; diluted 1:1000), anti-mouse-IL-6 (Servicebio, Wuhan, China; diluted 1:500), anti-β-actin (Affinity, Jiangsu, China; diluted 1:3000), and anti-β-tubulin (Affinity, Jiangsu, China; diluted 1:2000). The membranes underwent three washes with TBST for 5 minutes each, followed by a 60-minute incubation at room temperature with secondary antibodies (Proteintech, Wuhan, China; diluted 1:5000). After an additional three washes with TBST, the membranes were treated with an ECL exposure solution and subjected to chemiluminescence for protein visualization.

Immunofluorescence Staining in vitro

Following the established co-culture protocol, macrophages collected from the upper chamber were seeded onto sterile cell slides. Once cells adhered, the complete culture medium was removed, and cells were washed three times with PBS. Cells were then fixed in 4% paraformaldehyde at 4°C for 30 minutes, followed by three PBS washes. Permeabilization was achieved by incubating cells with Triton X-100 for 10 minutes, followed by three additional PBS washes. Subsequently, cells were blocked with 5% BSA for 30 minutes. Primary antibodies anti-p-STAT3 (Affinity, Jiangsu, China; diluted 1:50) and anti-p-p65 (Proteintech, Wuhan, China; diluted 1:50) were added and incubated overnight at 4°C. After three washes with PBS, corresponding fluorescent secondary antibodies (Proteintech, Wuhan, China; diluted 1:100) were added and incubated at room temperature for 60 minutes in the dark. Following three final PBS washes, cells were stained with DAPI for 5 minutes, washed with PBS, and imaged using a laser confocal microscope.

Statistical Analysis

Data analysis was performed using R software (version 4.2.2, https://www.r-project.org/) and GraphPad Prism 8.0 (GraphPad Software Inc., USA). Results are expressed as mean ± standard error of the mean for normally distributed data. One-way analysis of variance, followed by post hoc Tukey's multiple comparisons test, was conducted to compare

three or more groups, while Student's *t*-test was employed to compare two groups. Correlations between two variables were analyzed using Spearman or Pearson tests. Statistical significance was set at 0.05, with $*p < 0.05$, $**p < 0.01$, and $***p < 0.001$.

Results

Identification of DEGs and Functional Validation

Human cartilage samples from patients with OA and healthy controls were screened through the Gene Expression Omnibus (GEO) database (https://www.ncbi.nlm.nih.gov/geo/). Three microarray datasets (GSE178557, GSE183531, and GSE169077) were combined as the training set, while the RNA-seq dataset (GSE114007) served as the validation set. In the training set, 32 DEGs were identified, with 9 genes significantly upregulated and 23 genes significantly downregulated (Figure 1A). Candidate biomarker screening using machine learning was conducted with two distinct algorithms: LASSO and SVM-RFE. The LASSO regression algorithm identified 9 feature genes as diagnostic markers for OA (Figure 1B), while the SVM-RFE algorithm identified 25 feature genes (Figure 1C). Eight overlapping features (LOXL1, HILPDA, IRAK3, BEST1, HIST1H1C, CYP3A5, FAM65B, HSD11B1) were confirmed as OA-related biomarkers (Figure 1D), potentially playing crucial roles in OA progression.

Predicted Performance of Biomarkers

To further evaluate the predictive value of these eight potential biomarkers, ROC analysis was performed on the training dataset, revealing that all eight biomarkers exhibited an area under the curve (AUC) exceeding 0.8 for OA prediction (Figure 2A). The differential expression of these biomarkers was validated using the RNA-seq dataset GSE114007 (Figure 2B). In patients with OA compared to the control cohort, the expression trends of LOXL1, BEST1, HILPDA, HIST1H1C, and HSD11B1 mirrored those in the training set and showed significant disparities. Although the expression trends of CYP3A5, FAM65B, and IRAK3 remained consistent with the training group, no significant differences were observed. Furthermore, ROC analysis of these biomarkers in the validation group (Figure 2C) indicated that LOXL1, BEST1, HILPDA, HIST1H1C, and HSD11B1 had AUCs greater than 0.7 for predicting OA, indicating high predictive accuracy. However, the ROC analysis results for CYP3A5, FAM65B, and IRAK3 were unsatisfactory. Consequently, five hub biomarkers with OA-specific expression—LOXL1, BEST1, HILPDA, HIST1H1C, and HSD11B1—were identified. Given the elevated expression of LOXL1 in the cartilage of patients with OA and its superior predictive performance, LOXL1 was selected as the focal point for subsequent investigations.

Circulating LOXL1 Expression Was up-Regulated and Associated with Inflammatory Factors in Patients With OA

To confirm circulating LOXL1 levels in patients with OA, LOXL1 mRNA in whole blood and its protein in serum were detected. As shown in Figure 3A and B, the levels of LOXL1 mRNA and protein were elevated in patients with OA compared to the control group. Considering the critical role of inflammation in osteoarthritis, inflammatory cytokines in the serum of patients with OA were also assessed. Patients with OA exhibited higher levels of IL-6 and IL-8 compared to the control group (Figure 3C). Furthermore, LOXL1 levels positively correlated with IL-6 and IL-8 in the serum of patients with OA (Figure 3D). These findings suggest that LOXL1 from chondrocytes is highly expressed in patients with OA and is associated with the inflammatory response, indicating its potential as a marker of OA-related inflammation.

LOXL1 Was Highly Expressed in Cartilage and Associated with $iNOS^+$ M1 Macrophages in OA Rats

Considering the critical role of macrophages in OA inflammation, the expression of LOXL1 in cartilage, as well as $iNOS^+$ M1 and Arg^+ M2 macrophages in the synovium of OA rats, was examined. Consistent with serum analyses in patients with OA, a notable increase in LOXL1 and IL-6 levels within the cartilage of OA rats was observed, alongside an elevated presence of $iNOS^+$ M1 macrophages in the synovial tissue (Figure 4A–D). Additionally, LOXL1 levels positively correlated with the expression of IL-6 and iNOS (Figure 4E). These findings suggest that LOXL1 is associated

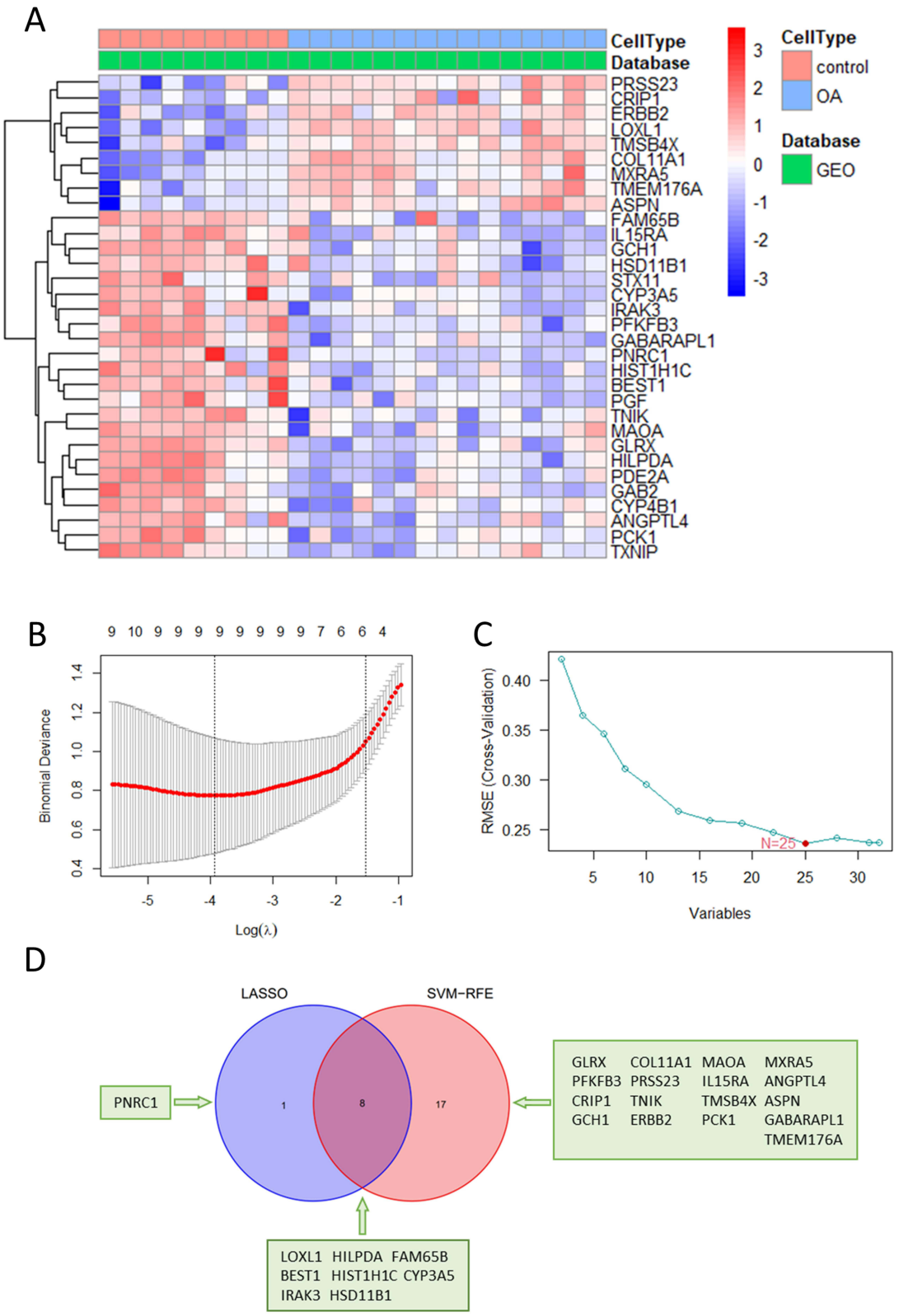

Figure 1 Identification of DEGs and selection of candidate biomarkers for OA via machine learning. (**A**) The heatmap presents the DEGs between OA and healthy specimens. (**B**) The LASSO logistic regression model retained the most predictive features. (**C**) Biomarkers were screened using the SVM-RFE algorithm. (**D**) The Venn diagram illustrates the intersection of biomarkers identified by both the LASSO logistic regression model and the SVM-RFE algorithm.

https://doi.org/10.2147/ITT.S512768

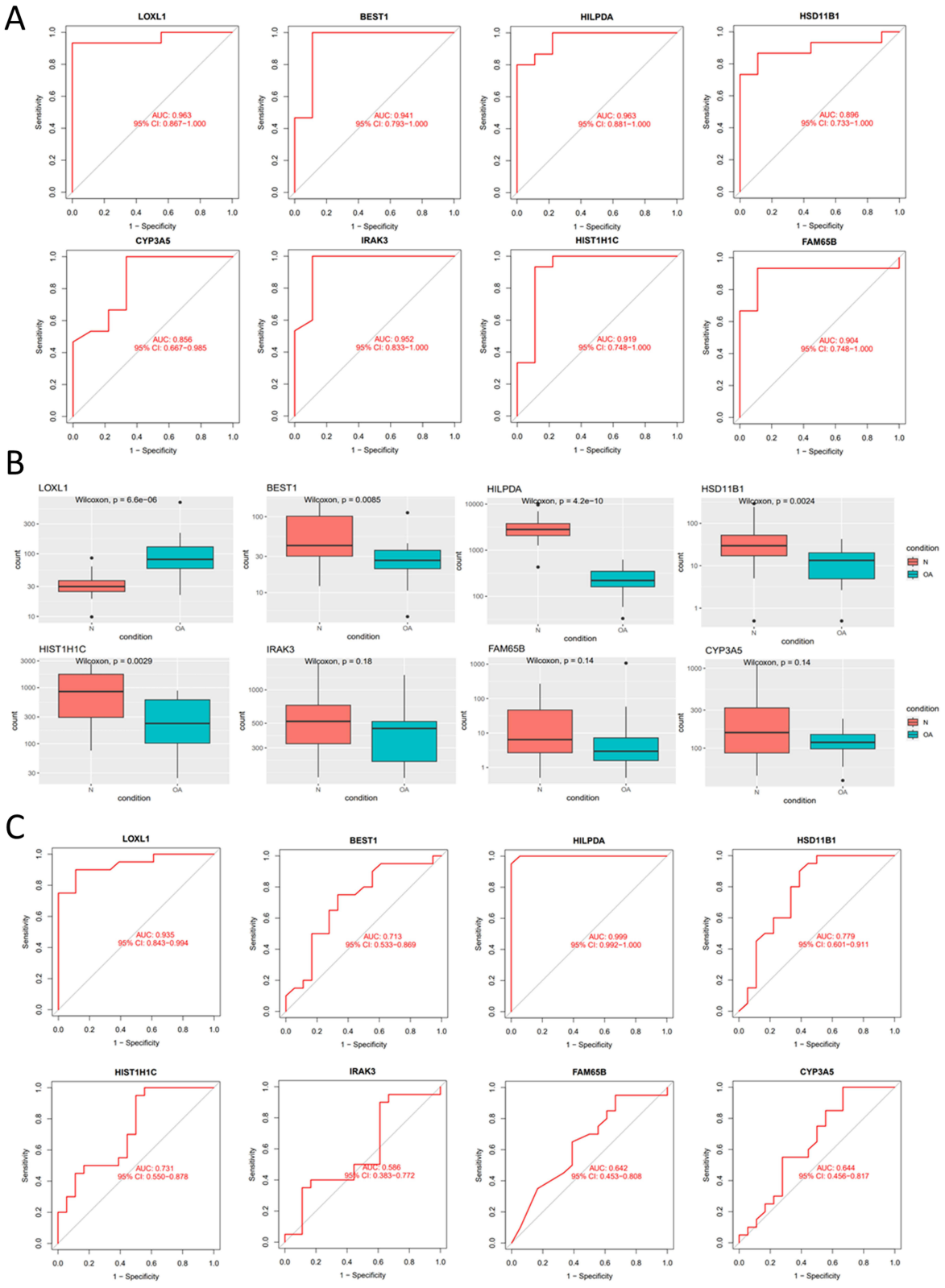

Figure 2 Predicted performance of biomarkers. (**A**) ROC curves of eight candidate biomarkers in the training set. (**B**) Differential expressions of candidate biomarkers in the validation set. (**C**) ROC curves of eight candidate biomarkers in the validation set.

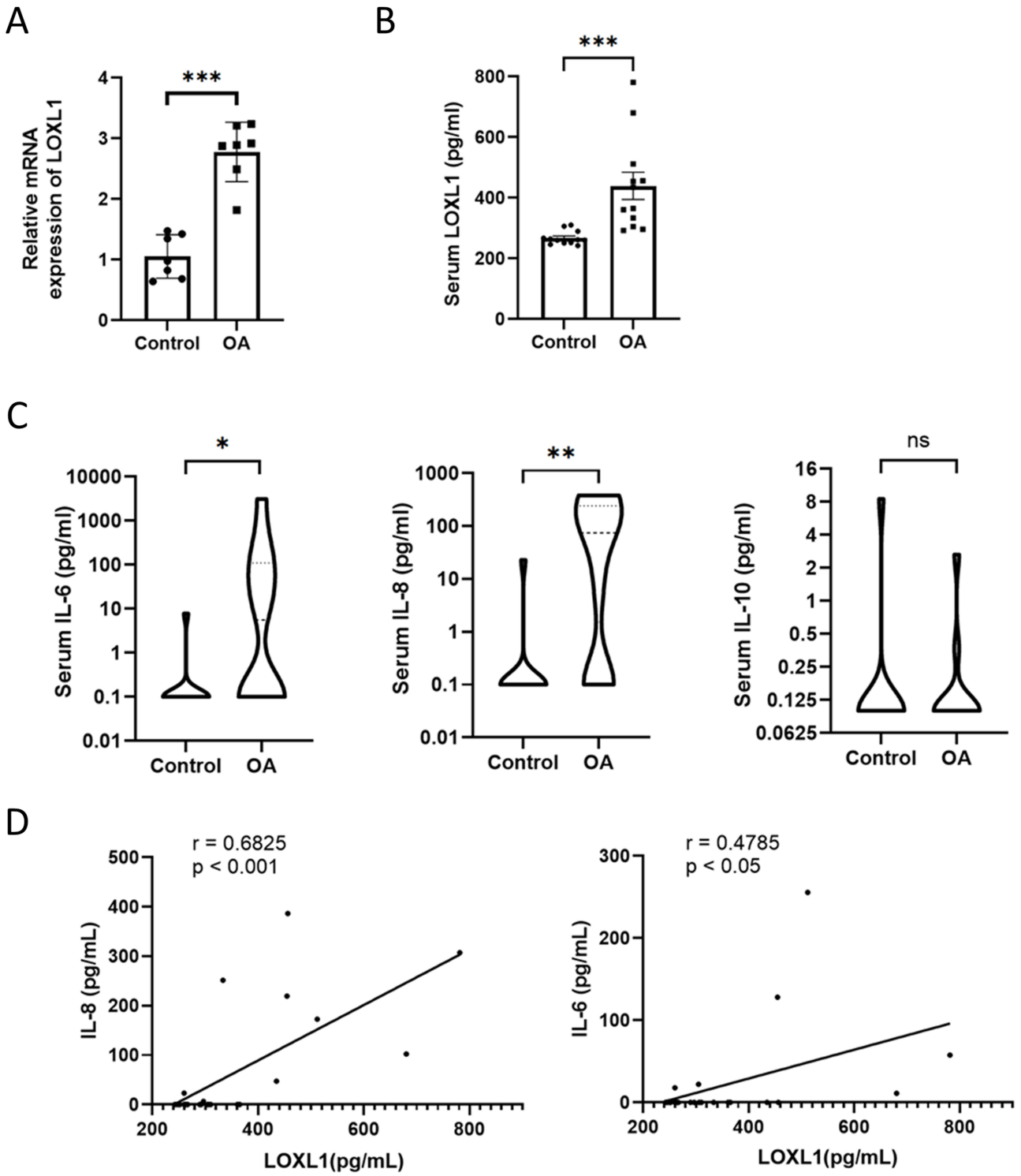

Figure 3 Patients with OA exhibited high expression of LOXL1, which was associated with circulating inflammatory cytokines. (**A**) mRNA expression levels of LOXL1 in whole blood samples from patients with OA and healthy controls. (**B**) Secretion levels of LOXL1 protein in the serum of patients with OA and healthy controls. (**C**) Secretion levels of IL-6, IL-8, and IL-10 in the serum of patients with OA and healthy controls. (**D**) Spearman correlation analysis between serum levels of LOXL1 and IL-6, IL-8. *$p < 0.05$, **$p < 0.01$, ***$p < 0.001$.

Abbreviation: ns, not significant.

https://doi.org/10.2147/ITT.S512768

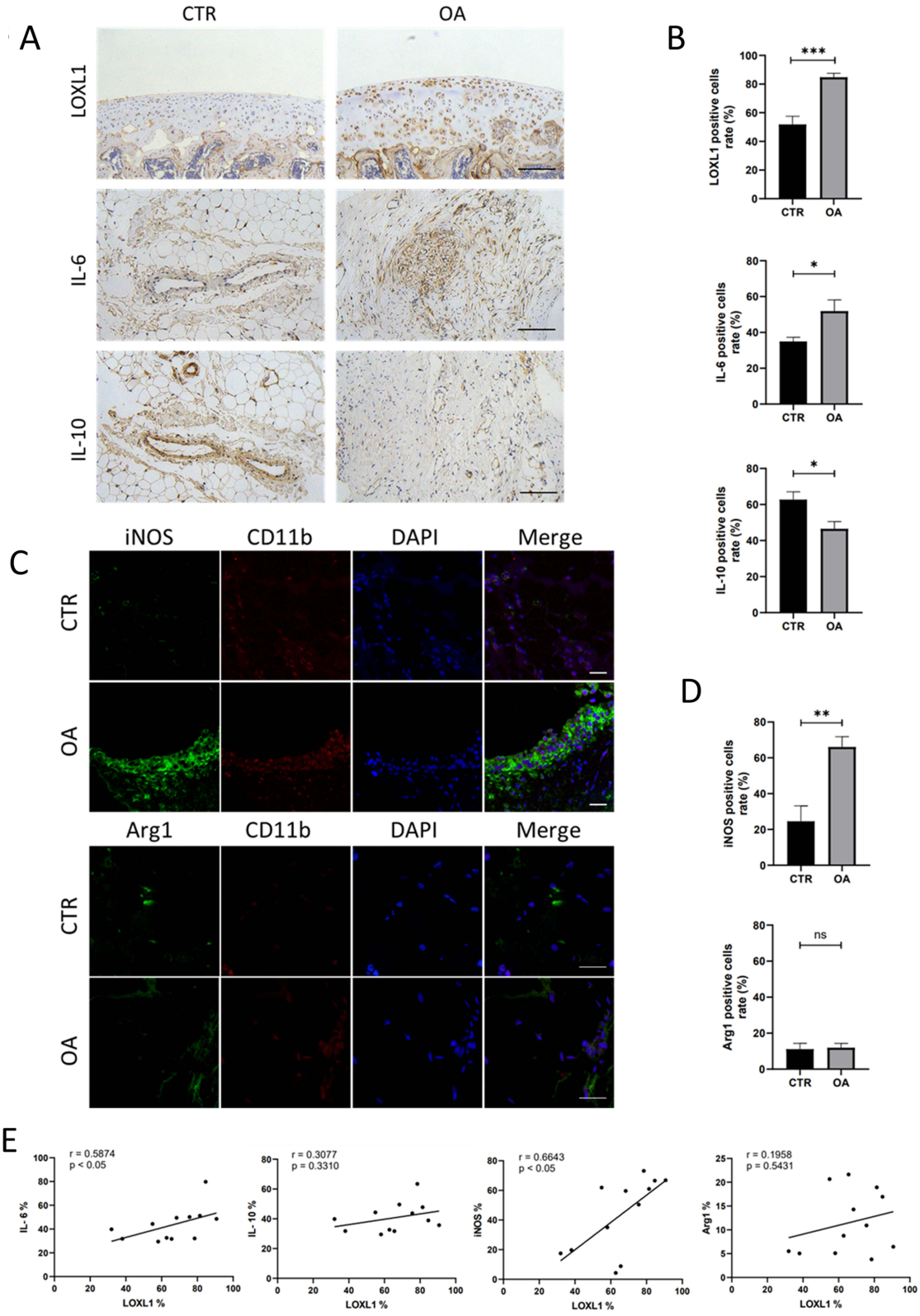

Figure 4 OA rats exhibited high expression of LOXL1 in joints, which was associated with inflammatory cytokines and iNOS$^+$ macrophages. (**A**) Representative images showing LOXL1 expression in cartilage, and IL-6 and IL-10 expression in the synovium of control and OA rat knee joints via immunohistochemistry analysis (scale bar = 100 μM). (**B**) Quantitative analysis of LOXL1, IL-6, and IL-10 expression. (**C**) Representative images of iNOS, Arg1, and CD11b expression in the synovium of control and OA rat knee joints via immunofluorescence analysis (scale bar = 25 μM). (**D**) Quantitative analysis of iNOS, Arg1, and CD11b expression. (**E**) Spearman correlation analysis of LOXL1 levels with IL-6, IL-10, iNOS, and Arg1 expression levels. *p < 0.05, **p < 0.01, ***p < 0.001.

Abbreviation: ns, not significant.

with M1 macrophages and inflammatory cytokines in OA rat joints, indicating that LOXL1 may contribute to the inflammatory response by promoting M1 macrophage activation in OA.

LOXL1 Activates M1 Macrophages in vitro

To investigate the effect of LOXL1 on macrophage activation, M0 macrophages were treated with recombinant LOXL1 protein in vitro, and their surface molecules and cytokine secretion were analyzed. As shown in Figure 5A, LOXL1-treated macrophages exhibited a mature phenotype with uropods and ruffles, contrasting with the immature round morphology observed in the control group. The expression of the M1-related marker CD86 increased, whereas the expression of the M2-related marker CD206 remained unchanged after LOXL1 treatment (Figure 5B and C). Additionally, the levels of IL-1β, IL-6, and TNF-α increased in LOXL1-treated macrophages compared to the control group (Figure 5D). These results suggest that LOXL1 stimulates M1 macrophage activation in vitro.

LOXL1 Knockdown Downregulates Cartilage Degradation Markers and Reduces Chondrocyte Apoptosis

To investigate LOXL1's pathophysiological role in chondrocytes, siRNA was used to inhibit its expression, verified through qRT-PCR and Western Blot analysis. Figures 6A–C demonstrate reduced LOXL1 levels in siRNA1 and siRNA2 samples. Subsequently, LOXL1 knockdown led to a significant decrease in MMP13 expression, indicating diminished cartilage degradation (Figure 6D and E), alongside a lower apoptosis rate (Figure 6F and G). These findings imply that LOXL1 downregulation in chondrocytes alleviates cartilage degradation and apoptosis, suggesting that LOXL1 promotes OA inflammation primarily via macrophage activation.

LOXL1 Knockdown in Chondrocytes Decreases the Activation of Macrophages

To examine the impact of chondrocyte-derived LOXL1 on macrophage activation, macrophages were co-cultured with LOXL1-knockdown chondrocytes, as depicted in the schematic diagram in Figure 7A. Figure 7B and C illustrate a significant reduction in the M1 marker CD86 expression in the LOXL1-siRNA1 and LOXL1-siRNA2 groups compared to the LOXL1-siCTR group. Although CD206 showed a slight increase, this change was negligible. Additionally, LOXL1-siRNA1 and LOXL1-siRNA2 groups displayed downregulated levels of IL-6, IL-8, and TNF-α, along with upregulated IL-10 levels, relative to the control group (Figure 7D). Furthermore, the supernatant from the LOXL1-siRNA1 and LOXL1-siRNA2 groups in the co-culture system exhibited lower LOXL1 secretion by macrophages compared to the control group (Figure 7E). Similarly, RAW264.7 cells were co-cultured with LOXL1-knockout chondrocytes, as shown in Figure 7F. Compared to the LOXL1-siCTRL group, the LOXL1-siRNA group exhibited a decrease in M1 marker CD86 expression, while M2 marker ARG1 remained unchanged. Furthermore, IL-6 and TNF-α levels were downregulated in the LOXL1-siRNA1 group relative to the control group, while IL-10 showed no significant change. Collectively, these findings suggest that LOXL1 silencing in chondrocytes diminishes the activation of co-cultured macrophages.

LOXL1 Activates M1 Macrophage via NF-κB and STAT3 Signaling

Given the role of STAT3 and NF-κB signaling pathways in the secretion of inflammatory cytokines that activate macrophages,[15,16] changes in these two pathways was analyzed in macrophages co-cultured with LOXL1-knockdown chondrocytes. Immunofluorescence and Western Blot results showed that the phosphorylation levels of the key transcription factors in the STAT3 and NF-κB signaling, p-STAT3 and p-p65, were inhibited in the LOXL1-siRNA group compared to the LOXL1-CTRL group (Figure 8A–D). Furthermore, LOXL1-treated macrophages upregulate NF-κB p65 phosphorylation, but the addition of NF-κB inhibitor SC75741 downregulates the expression of M1 marker CD86, TNF-α and IL-1β in a dose-dependent manner, with no effect on the expression of M2 marker Arg1 (Figure 8E). Similarly, LOXL1 treatment increases macrophage STAT3 phosphorylation, while STAT3 inhibitor Stattic decreases the expression of CD86, IL-6 and IL-1β, but has no effect on the expression of M2 marker Arg1 (Figure 8F). Furthermore, p-STAT3 and p-p65 were inhibited in RAW264.7 after co-cultured with LOXL1-siRNA chondrocytes (Figure 8G). However,

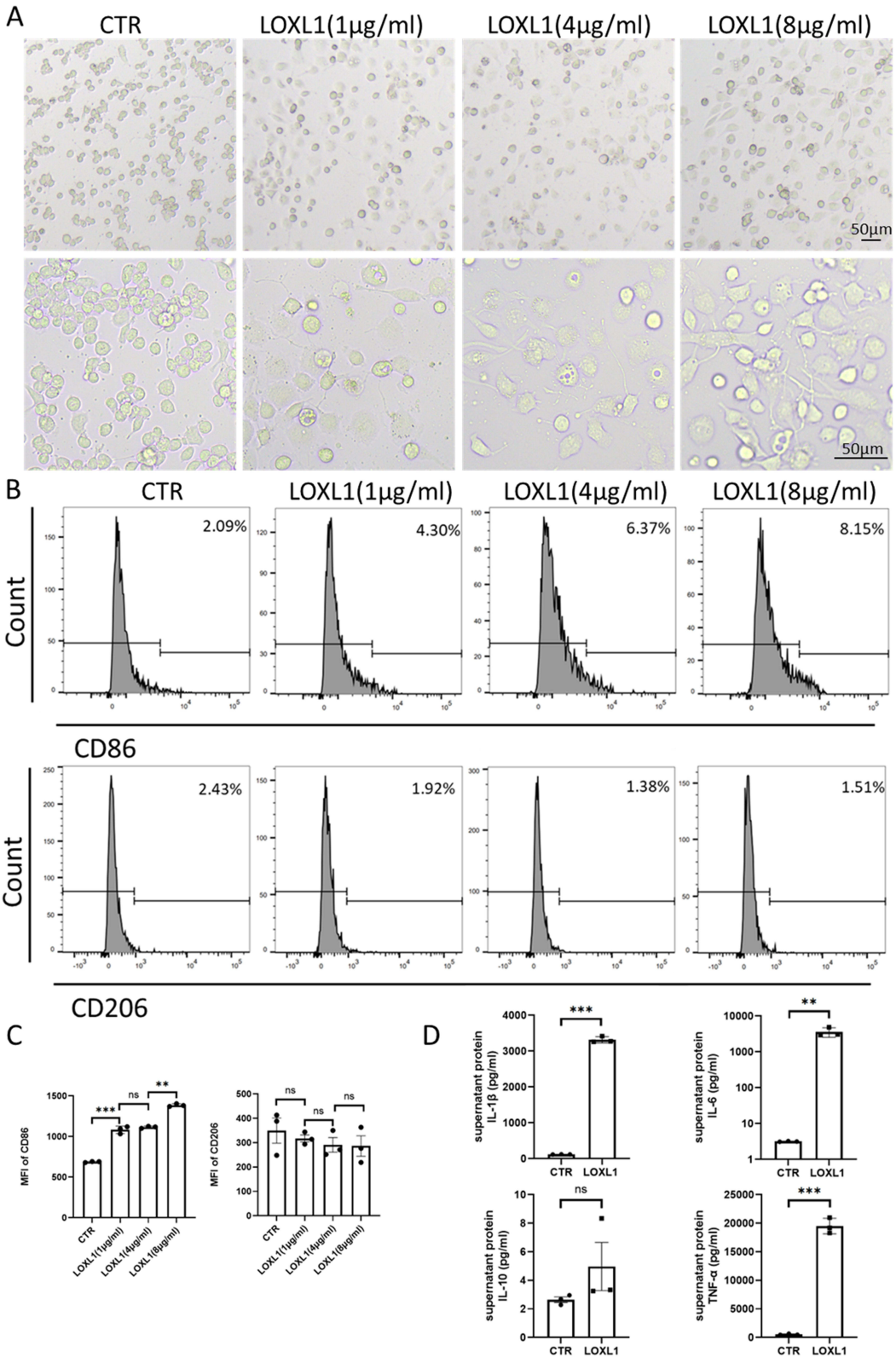

Figure 5 LOXL1 activates M1 macrophages in vitro. (**A**) Morphology of macrophages following different concentrations of LOXL1 stimulation (scale bar = 50 μM). (**B**) Representative FACS plots of CD86 and CD206. (**C**) Mean fluorescence intensity (MFI) of CD86 and CD206 on macrophages determined by flow cytometry analysis. (**D**) Secretion levels of IL-1β, IL-6, IL-10, and TNF-α in macrophages after LOXL1 stimulation with 8 μg/mL of LOXL1. $^{**}p < 0.01$, $^{***}p < 0.001$.
Abbreviation: ns, not significant.

 https://doi.org/10.2147/ITT.S512768

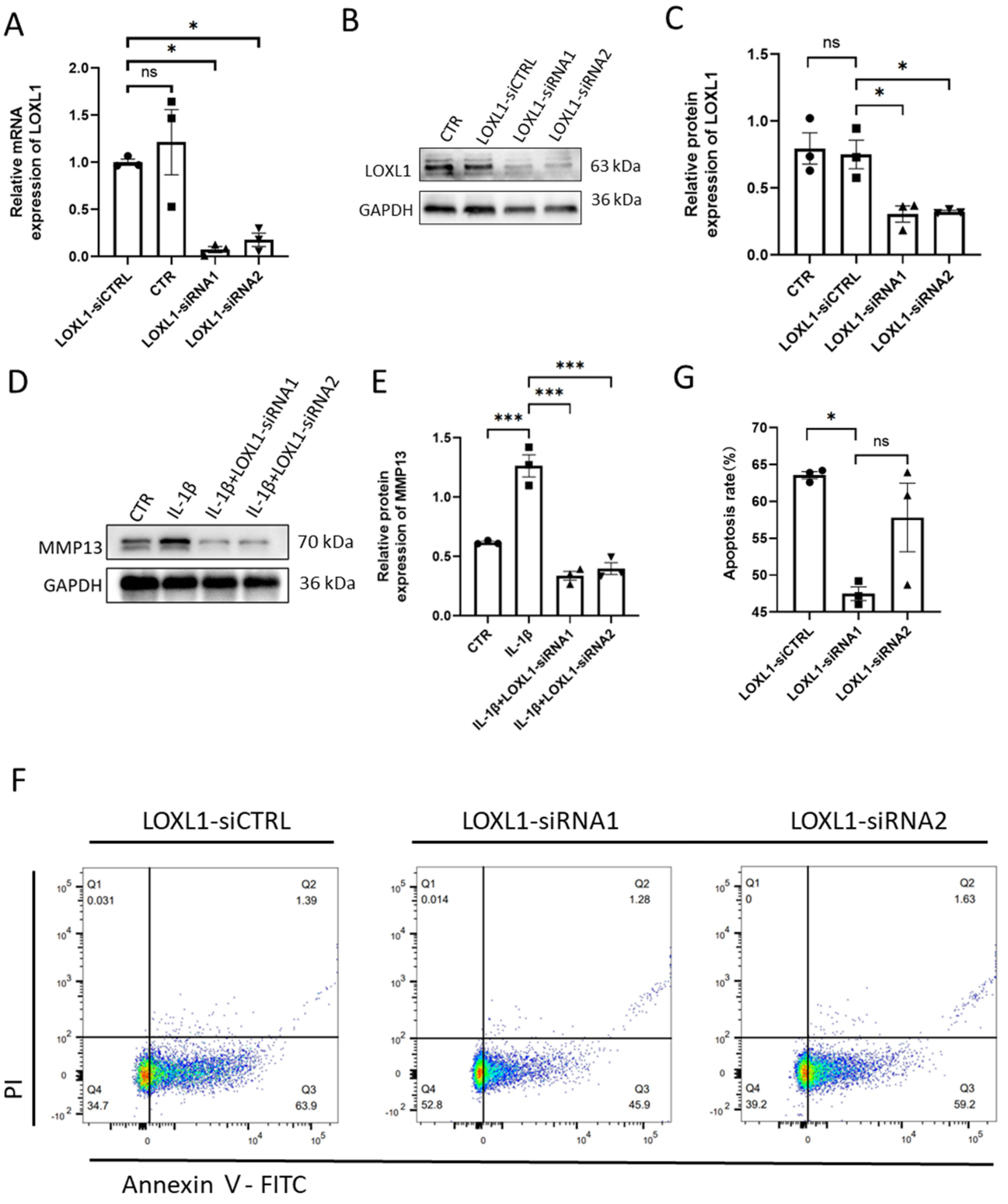

Figure 6 Silencing LOXL1 suppresses MMP13 expression and inhibits intrinsic apoptosis. (**A**) LOXL1 mRNA expression in chondrocytes after siRNA silencing, assessed by qRT-PCR. (**B** and **C**) LOXL1 protein expression in chondrocytes after siRNA silencing, determined by Western blotting. (**D**) Representative images of MMP13 expression in chondrocytes after LOXL1 silencing, shown by Western blotting. (**E**) Quantitative analysis of MMP13 expression in chondrocytes following LOXL1 silencing. (**F**) Representative FACS plots of chondrocyte apoptosis post-LOXL1 silencing. (**G**) Quantitative analysis of chondrocyte apoptosis after LOXL1 silencing. *$p < 0.05$, ***$p < 0.001$.
Abbreviation: ns, not significant.

https://doi.org/10.2147/ITT.S512768

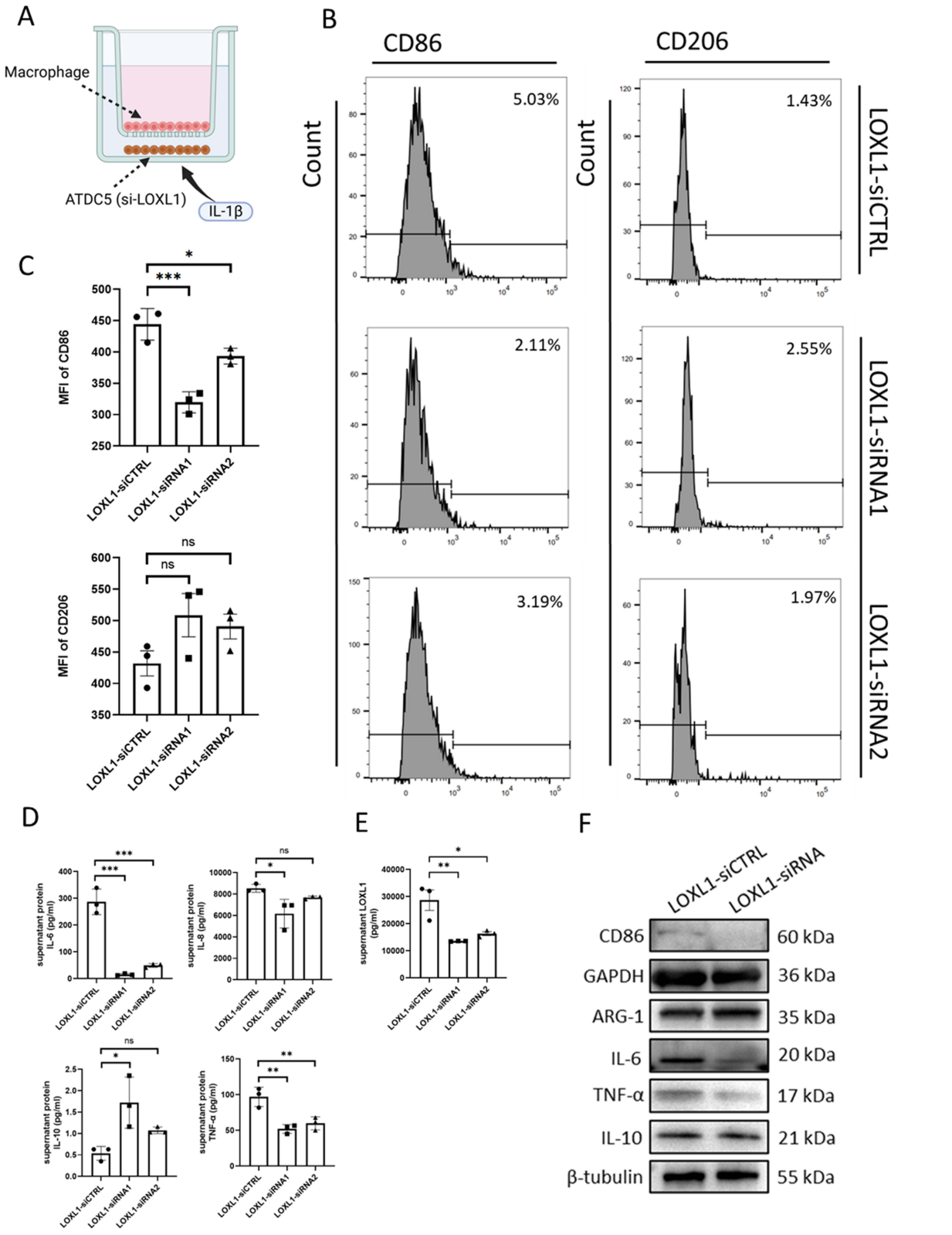

Figure 7 LOXL1 knockdown in chondrocytes decreases macrophage activation. (**A**) Schematic representation of the chondrocyte and macrophage co-culture model. (**B**) Representative FACS plots of CD86 and CD206. (**C**) MFI of CD86 and CD206 on macrophages determined by flow cytometry after LOXL1 knockdown in chondrocytes. (**D**) Secretion levels of IL-6, IL-8, IL-10, and TNF-α in macrophages co-cultured with chondrocytes following LOXL1 knockdown. (**E**) Secretion levels of LOXL1 in macrophages co-cultured with chondrocytes after LOXL1 knockdown. (**F**) Representative pictures of CD86, ARG1, IL-6, TNF-α and IL-10 expression in RAW264.7 co-cultured with chondrocytes following LOXL1 knockdown by WB. *$p < 0.05$, **$p < 0.01$, ***$p < 0.001$.
Abbreviation: ns, not significant.

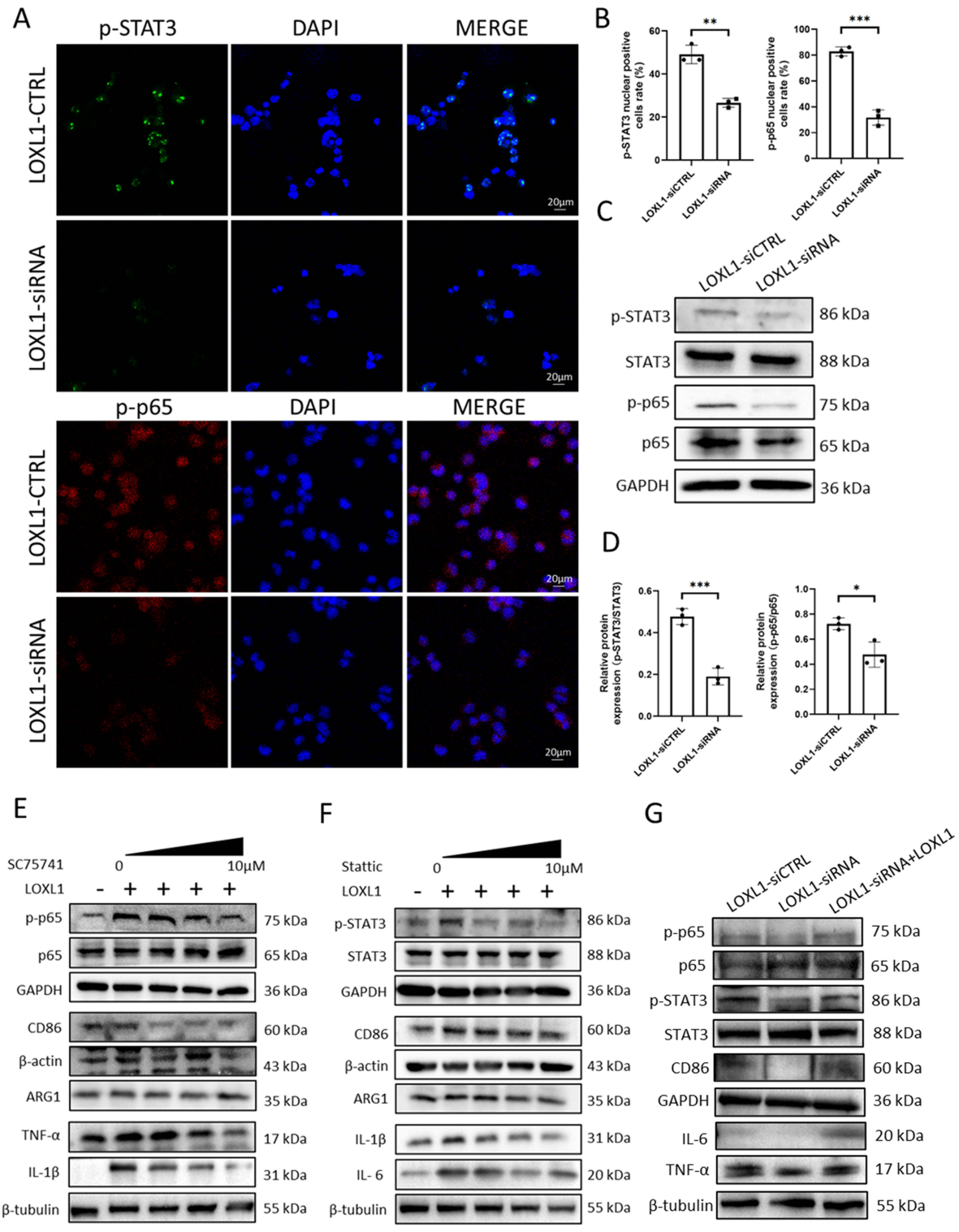

Figure 8 LOXL1-mediated macrophage polarization via NF-κB and STAT3 signaling pathways. (**A**) Representative pictures of p-STAT3 and p-p65 nuclear expression in macrophages co-cultured with chondrocytes following LOXL1 knockdown by immunofluorescence analysis (scale bar = 20 μM). (**B**) Quantitative analysis of p-STAT3 and p-p65 nuclear expression. (**C**) Representative pictures of the phosphorylation levels of STAT3 and p65 expression in macrophages co-cultured with chondrocytes following LOXL1 knockdown by WB. (**D**) Quantitative analysis of the phosphorylation levels of STAT3 and p65 expression. (**E**) Representative pictures of the phosphorylation levels of p65, CD86, ARG1, TNF-α and IL-1β expression in macrophages treated with LOXL1 and SC75741 by WB. (**F**) Representative pictures of the phosphorylation levels of STAT3, CD86, ARG1, IL-6 and IL-1β expression in macrophages treated with LOXL1 and Stattic by WB. (**G**) Representative pictures of the phosphorylation levels of STAT3 and p65, as well as CD86, IL-6 and TNF-α expression in RAW264.7 co-cultured with chondrocytes after LOXL1 knockdown, followed by LOXL1 supplementation by WB. *$p < 0.05$, **$p < 0.01$, ***$p < 0.001$.

Abbreviation: ns, not significant.

https://doi.org/10.2147/ITT.S512768

RAW264.7 cells co-cultured with LOXL1-knockdown chondrocytes were stimulated with recombinant mouse LOXL1 protein, an upregulation of phosphorylation levels of STAT3 and p65 in macrophages was observed, as well as an increase in M1 marker CD86 and pro-inflammatory cytokines TNF-α and IL-1β expression (Figure 8G). Thus, these results demonstrate that LOXL1 promotes M1 macrophage activation via STAT3 and NF-κB signaling.

Discussion

The diagnosis of OA relies on clinical symptoms combined with radiographic findings, such as joint space narrowing, bone cysts, bone sclerosis, and osteophyte development, typically seen at advanced and often irreversible stages.[17,18] Consequently, OA treatment remains largely palliative. The search for biomarkers to diagnose OA and predict its progression has gained significant attention.[19] However, current markers based on cartilage degradation, including type II collagen markers, hyaluronic acid, and matrix metalloproteinases, often do not correlate consistently with the radiological progression of OA.[20] Elevated levels of high-sensitivity C-reactive protein (hsCRP) in the early stages of OA suggest that inflammation plays a role in the early pathophysiology of the disease.[21] Early identification of inflammatory biomarkers in OA and timely intervention can delay cartilage and bone damage, thereby reducing clinical disability. Thus, inflammatory biomarkers for OA are promising both for screening and as a treatment cornerstone.

In this study, eight genes (LOXL1, HILPDA, IRAK3, BEST1, HIST1H1C, CYP3A5, FAM65B, and HSD11B1) were identified as specific markers for OA using bioinformatics algorithms on public databases (GSE178557, GSE183531, and GSE169077). Subsequent validation with the GSE114007 dataset confirmed five genes (LOXL1, HSD11B1, BEST1, HILPDA, and HIST1H1) exhibiting trends consistent with those in the training dataset. Immune infiltration analysis revealed that NK cells and macrophages particularly infiltrate the cartilage of patients with OA (data not shown). Given the pivotal role of macrophages in initiating and sustaining inflammation in OA,[22,23] it is inferred that LOXL1 may contribute to the OA inflammatory response through its interaction with macrophages.

LOXL1 is expressed in elastic tissues, including the aorta, uterus, and lungs.[24,25] Aberrant LOXL1 expression is implicated in various pathological processes related to the imbalance between ECM synthesis and degradation, such as idiopathic pulmonary fibrosis,[26] pseudoexfoliation glaucoma,[12,27] and pseudoexfoliation syndrome.[12,28] Additionally, LOXL1 plays a dual role in tumor formation, either promoting or inhibiting it.[29] High LOXL1 expression is associated with invasive and metastatic traits in papillary thyroid cancer and lung cancer cells,[30,31] while it suppresses invasion and metastasis in colorectal and prostate cancer cells.[32,33] However, the expression and role of LOXL1 in osteoarthritis (OA) remain unexplored. Our study found that the LOXL1 gene has an impressive area under the curve (AUC) of 0.963 (95% CI 0.867–1.000) in predicting OA, as revealed by ROC analysis. Transcriptome RNA-seq datasets further confirmed elevated LOXL1 expression in patients with OA. Moreover, LOXL1 gene and protein levels were significantly higher in patients with OA compared to healthy controls, correlating positively with inflammatory cytokines IL-6 and IL-8 in the serum of patients with OA. These findings suggest that LOXL1 is a potential biomarker reflecting the inflammatory response in patients with OA. Interestingly, recent studies have shown that LOXL1 expression is upregulated in the synovium of patients with rheumatoid arthritis, and that knocking down LOXL1 can inhibit synovial inflammation.[34]

Given the critical role of macrophages in OA inflammation, we analyzed the relationship between LOXL1 expression and macrophages in an osteoarthritis rat model. Results indicated increased expression of LOXL1 and IL-6 in the cartilage of osteoarthritis rats and a rise in $iNOS^+$ M1 macrophages in the synovium. LOXL1 expression correlated positively with IL-6 and iNOS levels. M1 macrophages, characterized by their pro-inflammatory phenotype, secrete cytokines such as TNF-α, IL-1β, and IL-6, which stimulate chondrocytes to produce ECM-degrading enzymes, exacerbating cartilage matrix degradation and perpetuating OA inflammation and progression.[35,36] The presence of M1 macrophages in the synovial fluid of OA joints is positively associated with clinical symptoms like stiffness and pain.[37] Conversely, M2 macrophages exhibit an anti-inflammatory phenotype, and the imbalance of increased M1 and decreased M2 macrophages is directly related to OA severity.[38,39] Moreover, activated macrophages are detectable at early OA stages,[40] and M1 macrophages accelerate OA progression in mice.[41] LOXL1 stimulated macrophages to increase the expression of the M1 marker CD86, without affecting the M2 marker CD206, and increased the secretion of IL-1β, IL-6, and TNF-α by macrophages in vitro. These results suggest that LOXL1 activates M1 macrophages, enhances the secretion of inflammatory cytokines, and participates in the inflammatory response of OA.

To assess the impact of LOXL1 on chondrocytes, LOXL1 was silenced using siRNA. This intervention led to reduced expression of the chondrocyte degradation marker MMP-13 and decreased chondrocyte apoptosis, suggesting that LOXL1 silencing enhances the biological function of chondrocytes. The pro-inflammatory effects of LOXL1 are likely related to macrophage activation. Understanding the crosstalk between chondrocytes and synovial macrophages in the occurrence and progression of OA not only elucidates OA pathogenesis but also facilitates the development of novel therapeutic interventions. To investigate macrophage activation by chondrocyte-expressed LOXL1, LOXL1 was knocked down in chondrocytes, which were then co-cultured with macrophages. The co-culture resulted in increased macrophage CD86 expression and elevated levels of IL-1β and IL-6. However, LOXL1 knockdown in chondrocytes led to reduced CD86 expression and lower secretion of inflammatory cytokines in macrophages, indicating that chondrocyte-derived LOXL1 can activate M1 macrophages and promote inflammatory cytokine secretion.

NF-κB signaling is an important transcription factor for macrophage activation, which regulates the secretion of a variety of inflammatory cytokines and participates in inflammatory responses.[23,42,43] Moreover, NF-κB is involved in OA pathology in a variety of patterns.[44] For example, NF-κB signaling induces the secretion of various matrix metalloproteinases such as MMP1, MMP9 and MMP13, causing articular cartilage degeneration.[45] NF-κB-mediated secretion of IL-1β, IL-6 and TNF-α not only participates in OA inflammation, but also induces the production of MMPs, and aggravates the destruction of OA articular cartilage.[46,47] Similarly, STAT3 signaling is also involved in macrophage polarization.[48] STAT3 is regulated by a variety of cytokines and growth factors through JAK/STAT signaling, and is involved in the inflammatory and immune responses of a variety of diseases.[48,49] Although JAK/STAT3 signaling activation promotes M2 macrophage polarization in tumors,[50] JAK2/STAT3 activity increases in inflammation, inhibits JAK/STAT3 signaling, and promotes M2 macrophage polarization in pancreatitis and psoriasis.[51,52] However, JAK2/STAT3 plays an important role in the initiation and progression of OA.[53] High expression of JAK2/STAT3 signaling in osteoarthritis cartilage tissue, and high expression of JAK2 and STAT3 reduce COL II level, resulting in cartilage matrix damage.[54] In addition, proinflammatory cytokines released by chondrocytes or synovial cells, such as IL-1β and IL-6, can regulate the JAK2/STAT3 pathway and initiate the OA inflammatory response.[55,56] Whether chondrocyte-derived LOXL1 stimulates M1 macrophage activation is mediated by NF-κB and STAT3 signaling. As expected, LOXL1 knockdown in chondrocytes reduces NF-κB p-p65 and p-STAT3 expression in co-cultured macrophages. In addition, LOXL1-stimulated macrophages increase p-p65 and p-STAT3 expression, and LOXL1 in combination with NF-κB or STAT3 inhibition, decreases NF-κB and STAT3 activation, and decreases CD86 and IL-1β, TNF-α or IL-6 expression. Thus, chondrocyte-derived LOXL1 activates macrophages through NF-κB and STAT3 pathways, leading to increased inflammatory cytokine secretion.

Synovitis in OA is primarily driven by macrophages,[57] and the number of folate receptor (FR)-positive macrophages in the joint correlates with the severity and symptoms of radiographic knee OA. Etarfolatide (EC20) imaging identifies the inflammatory phenotype in OA patients in vivo by characterizing the expression of FR on activated macrophages.[58] However, EC20 imaging involves radiation exposure. Therefore, identifying a soluble biomarker for activated macrophages could provide a way to recognize an inflammatory OA phenotype.[59] Given that LOXL1 derived from chondrocytes activates M1 macrophages, it is necessary to further evaluate whether LOXL1 can be used for OA inflammatory phenotyping, whether it activates OA macrophages, and whether it mediates joint structural progression.

Additionally, current OA management primarily focuses on pain relief and reducing inflammation, rather than repairing cartilage defects or restoring normal joint function.[60] Therefore, delaying degradation due to chondrocyte senescence and decreasing the inflammatory polarization of synovial macrophages could help cure OA. This also has significant implications for the development of new therapeutic strategies and effective drugs.[61] Given that LOXL1 knockdown reduces chondrocyte degradation and apoptosis and decreases M1 macrophage activation, targeting LOXL1 inhibition may offer a novel approach to prevent chondrocyte degradation and suppress macrophage-mediated inflammation. Thus, LOXL1 is identified not only as a potential marker of OA inflammation but also as a promising therapeutic target for OA management.

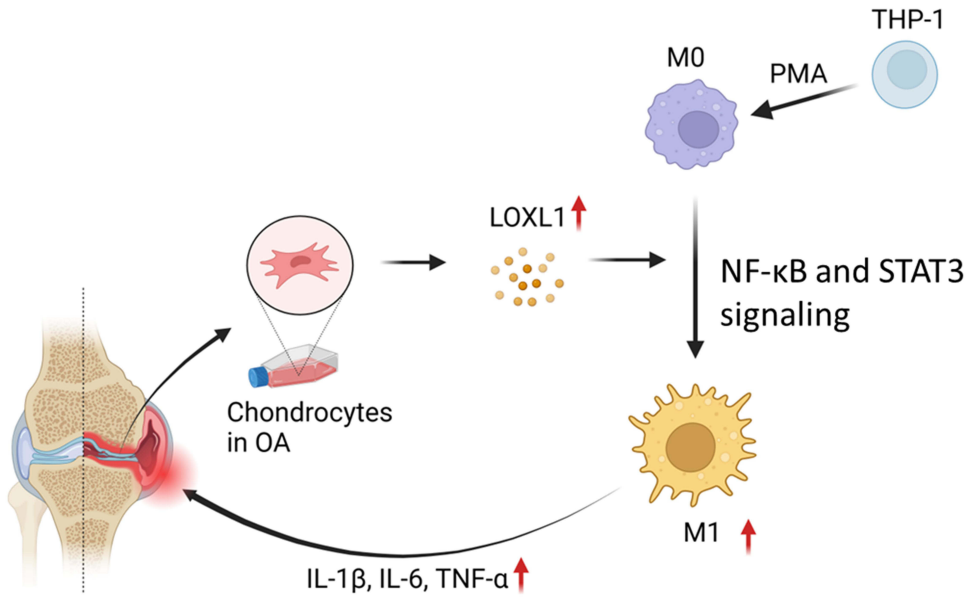

Figure 9 Schematic diagram illustrating the hypothetical role of LOXL1 in osteoarthritis (OA). Highly expressed LOXL1 in chondrocytes stimulates macrophage activation, leading to the production of inflammatory cytokines IL-1β, IL-6, and TNF-α via the STAT3 and NF-κB pathway. This activation accelerates chondrocyte degeneration and exacerbates OA inflammation.

Conclusion

This study identified that chondrocyte LOXL1 is highly expressed in patients with OA and is associated with inflammatory cytokines. LOXL1 primarily activates M1 macrophages via the NF-κB and STAT3 pathways, promoting the secretion of inflammatory cytokines and contributing to OA pathogenesis (Figure 9). Consequently, LOXL1 holds promise as a potential marker for early diagnosis of OA inflammation and as a novel therapeutic target.

Acknowledgment

We thank BioRender.com for the creation of Figures. We would like to thank EditChecks (https://editchecks.com.cn/) for providing linguistic assistance during the preparation of this manuscript. This work was supported by a grant from the National Natural Science Foundation of China (81871243), the key research and development programs of Jiangsu Province (BE2017697), the Six Talent Peaks of Jiangsu Province (WSN-009), and Zhenjiang Clinical Research Center of Gynecological Diseases of Traditional Chinese Medicine (SS202204-KFB02).

Author Contributions

All authors made a significant contribution to the work reported, whether that is in the conception, study design, execution, acquisition of data, analysis and interpretation, or in all these areas; took part in drafting, revising or critically reviewing the article; gave final approval of the version to be published; have agreed on the journal to which the article has been submitted; and agree to be accountable for all aspects of the work.

Disclosure

The authors report no conflicts of interest in this work.

References

1. Hamasaki M, Terkawi MA, Onodera T, Homan K, Iwasaki N. A Novel Cartilage Fragments Stimulation Model Revealed that Macrophage Inflammatory Response Causes an Upregulation of Catabolic Factors of Chondrocytes In Vitro. *Cartilage*. 2021;12(3):354–361. doi:10.1177/1947603519828426
2. Wang M, Tan G, Jiang H, et al. Molecular crosstalk between articular cartilage, meniscus, synovium, and subchondral bone in osteoarthritis. *Bone Joint Res*. 2022;11(12):862–872. doi:10.1302/2046-3758.1112.Bjr-2022-0215.R1

3. Li Z, Huang Z, Bai L. Cell Interplay in Osteoarthritis. *Front Cell Develop Biol*. 2021;9:720477. doi:10.3389/fcell.2021.720477
4. Rousseau J, Garnero P. Biological markers in osteoarthritis. *Bone*. 2012;51(2):265–277. doi:10.1016/j.bone.2012.04.001
5. Chou CH, Jain V, Gibson J, et al. Synovial cell cross-talk with cartilage plays a major role in the pathogenesis of osteoarthritis. *Sci Rep*. 2020;10 (1):10868. doi:10.1038/s41598-020-67730-y
6. Robinson WH, Lepus CM, Wang Q, et al. Low-grade inflammation as a key mediator of the pathogenesis of osteoarthritis. *Nat Rev Rheumatol*. 2016;12(10):580–592. doi:10.1038/nrrheum.2016.136
7. Pak J, Lee JH, Park KS, Park M, Kang LW, Lee SH. Current use of autologous adipose tissue-derived stromal vascular fraction cells for orthopedic applications. *J Biomed Sci*. 2017;24(1):9. doi:10.1186/s12929-017-0318-z
8. Sanchez-Lopez E, Coras R, Torres A, Lane NE, Guma M. Synovial inflammation in osteoarthritis progression. *Nat Rev Rheumatol*. 2022;18 (5):258–275. doi:10.1038/s41584-022-00749-9
9. Samavedi S, Diaz-Rodriguez P, Erndt-Marino JD, Hahn MS. A Three-Dimensional Chondrocyte-Macrophage Coculture System to Probe Inflammation in Experimental Osteoarthritis. *Tissue Eng Part A*. 2017;23(3–4):101–114. doi:10.1089/ten.TEA.2016.0007
10. Takahashi A, de Andrés MC, Hashimoto K, Itoi E, Oreffo RO. Epigenetic regulation of interleukin-8, an inflammatory chemokine, in osteoarthritis. *Osteoarthritis Cartilage*. 2015;23(11):1946–1954. doi:10.1016/j.joca.2015.02.168
11. Vallet SD, Ricard-Blum S. Lysyl oxidases: from enzyme activity to extracellular matrix cross-links. *Essays Biochem*. 2019;63(3):349–364. doi:10.1042/ebc20180050
12. Schlötzer-Schrehardt U, Zenkel M. The role of lysyl oxidase-like 1 (LOXL1) in exfoliation syndrome and glaucoma. *Exp Eye Res*. 2019;189:107818. doi:10.1016/j.exer.2019.107818
13. Yuan R, Li Y, Yang B, et al. LOXL1 exerts oncogenesis and stimulates angiogenesis through the LOXL1-FBLN5/αvβ3 integrin/FAK-MAPK axis in ICC. *mol Ther Nucleic Acids*. 2021;23:797–810. doi:10.1016/j.omtn.2021.01.001
14. Yi B, Li H, Cai H, Lou X, Yu M, Li Z. LOXL1-AS1 communicating with TIAR modulates vasculogenic mimicry in glioma via regulation of the miR-374b-5p/MMP14 axis. *J Cell & Mol Med*. 2022;26(2):475–490. doi:10.1111/jcmm.17106
15. Mantsounga CS, Lee C, Neverson J, et al. Macrophage IL-1β promotes arteriogenesis by autocrine STAT3- and NF-κB-mediated transcription of pro-angiogenic VEGF-A. *Cell Rep*. 2022;38(5):110309. doi:10.1016/j.celrep.2022.110309
16. Guo H, Jin D, Chen X. Lipocalin 2 is a regulator of macrophage polarization and NF-κB/STAT3 pathway activation. *Mol Endocrinol*. 2014;28 (10):1616–1628. doi:10.1210/me.2014-1092
17. Boffa A, Merli G, Andriolo L, Lattermann C, Salzmann GM, Filardo G. Synovial Fluid Biomarkers in Knee Osteoarthritis: a Systematic Review and Quantitative Evaluation Using BIPEDs Criteria. *Cartilage*. 2021;13(1_suppl):82s–103s. doi:10.1177/1947603520942941
18. Mobasheri A, Thudium CS, Bay-Jensen AC, et al. Biomarkers for osteoarthritis: current status and future prospects. *Best Pract Res*. 2023;37 (2):101852. doi:10.1016/j.berh.2023.101852
19. Bay-Jensen AC, Engstroem A, Sharma N, Karsdal MA. Blood and urinary collagen markers in osteoarthritis: markers of tissue turnover and disease activity. *Expert Review of Molecular Diagnostics*. 2020;20(1):57–68. doi:10.1080/14737159.2020.1704257
20. Jordan KM, Syddall HE, Garnero P, et al. Urinary CTX-II and glucosyl-galactosyl-pyridinoline are associated with the presence and severity of radiographic knee osteoarthritis in men. *Ann Rheumatic Dis*. 2006;65(7):871–877. doi:10.1136/ard.2005.042895
21. Jin X, Beguerie JR, Zhang W, et al. Circulating C reactive protein in osteoarthritis: a systematic review and meta-analysis. *Ann Rheumatic Dis*. 2015;74(4):703–710. doi:10.1136/annrheumdis-2013-204494
22. Thomson A, Hilkens CMU. Synovial Macrophages in Osteoarthritis: the Key to Understanding Pathogenesis? *Front Immunol*. 2021;12:678757. doi:10.3389/fimmu.2021.678757
23. Zhang H, Cai D, Bai X. Macrophages regulate the progression of osteoarthritis. *Osteoarthritis Cartilage*. 2020;28(5):555–561. doi:10.1016/j.joca.2020.01.007
24. Nave AH, Mižíková I, Niess G, et al. Lysyl oxidases play a causal role in vascular remodeling in clinical and experimental pulmonary arterial hypertension. *Arteriosclerosis Thrombosis Vasc Biol*. 2014;34(7):1446–1458. doi:10.1161/atvbaha.114.303534
25. Tjin G, White ES, Faiz A, et al. Lysyl oxidases regulate fibrillar collagen remodelling in idiopathic pulmonary fibrosis. *Dis Models Mech*. 2017;10 (11):1301–1312. doi:10.1242/dmm.030114
26. Bellaye PS, Shimbori C, Upagupta C, et al. Lysyl Oxidase-Like 1 Protein Deficiency Protects Mice from Adenoviral Transforming Growth Factor-β1-induced Pulmonary Fibrosis. *Am J Respir Cell mol Biol*. 2018;58(4):461–470. doi:10.1165/rcmb.2017-0252OC
27. Greene AG, Eivers SB, McDonnell F, Dervan EWJ, O'Brien CJ, Wallace DM. Differential Lysyl oxidase like 1 expression in pseudoexfoliation glaucoma is orchestrated via DNA methylation. *Exp Eye Res*. 2020;201:108349. doi:10.1016/j.exer.2020.108349
28. Greene AG, Eivers SB, Dervan EWJ, O'Brien CJ, Wallace DM. Lysyl Oxidase Like 1: biological roles and regulation. *Exp Eye Res*. 2020;193:107975. doi:10.1016/j.exer.2020.107975
29. Wang W, Wang X, Yao F, Huang C. Lysyl Oxidase Family Proteins: prospective Therapeutic Targets in Cancer. *Int J mol Sci*. 2022;23(20):12270. doi:10.3390/ijms232012270
30. Meng K, Hu X, Zheng G, et al. Identification of prognostic biomarkers for papillary thyroid carcinoma by a weighted gene co-expression network analysis. *Cancer Med*. 2022;11(9):2006–2019. doi:10.1002/cam4.4602
31. Lee GH, Kim DS, Chung MJ, Chae SW, Kim HR, Chae HJ. Lysyl oxidase-like-1 enhances lung metastasis when lactate accumulation and monocarboxylate transporter expression are involved. *Oncol Lett*. 2011;2(5):831–838. doi:10.3892/ol.2011.353
32. Hu L, Wang J, Wang Y, et al. LOXL1 modulates the malignant progression of colorectal cancer by inhibiting the transcriptional activity of YAP. *CCS*. 2020;18(1):148. doi:10.1186/s12964-020-00639-1
33. Wang W, Yuan D, Jiang K, et al. Genome-Wide CRISPR-Cas9 Screening and Identification of Potential Genes Promoting Prostate Cancer Growth and Metastasis. *Curr Cancer Drug Targets*. 2022;23(1):71–86. doi:10.2174/1568009622666220615154137
34. Hu J, Liu X, Xu Q, et al. Mechanism of lysine oxidase-like 1 promoting synovial inflammation mediating rheumatoid arthritis development. *Aging*. 2024;16(1):928–947. doi:10.18632/aging.205429
35. Wu CL, Harasymowicz NS, Klimak MA, Collins KH, Guilak F. The role of macrophages in osteoarthritis and cartilage repair. *Osteoarthritis Cartilage*. 2020;28(5):544–554. doi:10.1016/j.joca.2019.12.007
36. Deng C, Xiao Y, Zhao X, et al. Sequential Targeting Chondroitin Sulfate-Bilirubin Nanomedicine Attenuates Osteoarthritis via Reprogramming Lipid Metabolism in M1 Macrophages. *Adv Sci*. 2025;12(9):e2411911. doi:10.1002/advs.202411911

37. Sakurai Y, Fujita M, Kawasaki S, et al. Contribution of synovial macrophages to rat advanced osteoarthritis pain resistant to cyclooxygenase inhibitors. *Pain*. 2019;160(4):895–907. doi:10.1097/j.pain.0000000000001466
38. Zhang H, Lin C, Zeng C, et al. Synovial macrophage M1 polarisation exacerbates experimental osteoarthritis partially through R-spondin-2. *Ann Rheumatic Dis*. 2018;77(10):1524–1534. doi:10.1136/annrheumdis-2018-213450
39. Liu B, Zhang M, Zhao J, Zheng M, Yang H. Imbalance of M1/M2 macrophages is linked to severity level of knee osteoarthritis. *Exp Ther Med*. 2018;16(6):5009–5014. doi:10.3892/etm.2018.6852
40. Piscaer TM, Müller C, Mindt TL, et al. Imaging of activated macrophages in experimental osteoarthritis using folate-targeted animal single-photon-emission computed tomography/computed tomography. *Arthritis Rheum*. 2011;63(7):1898–1907. doi:10.1002/art.30363
41. Blom AB, van Lent PL, Holthuysen AE, et al. Synovial lining macrophages mediate osteophyte formation during experimental osteoarthritis. *Osteoarthritis Cartilage*. 2004;12(8):627–635. doi:10.1016/j.joca.2004.03.003
42. Zheng Y, Wei K, Jiang P, et al. Macrophage polarization in rheumatoid arthritis: signaling pathways, metabolic reprogramming, and crosstalk with synovial fibroblasts. *Front Immunol*. 2024;15:1394108. doi:10.3389/fimmu.2024.1394108
43. Sun Y, Zuo Z, Kuang Y. An Emerging Target in the Battle against Osteoarthritis: macrophage Polarization. *Int J mol Sci*. 2020;21(22):8513. doi:10.3390/ijms21228513
44. Yao Q, Wu X, Tao C, et al. Osteoarthritis: pathogenic signaling pathways and therapeutic targets. *Signal Transduct Targeted Ther*. 2023;8(1):56. doi:10.1038/s41392-023-01330-w
45. Ulivi V, Giannoni P, Gentili C, Cancedda R, Descalzi F. p38/NF-kB-dependent expression of COX-2 during differentiation and inflammatory response of chondrocytes. *J Cell Biochem*. 2008;104(4):1393–1406. doi:10.1002/jcb.21717
46. Kapoor M, Martel-Pelletier J, Lajeunesse D, Pelletier JP, Fahmi H. Role of proinflammatory cytokines in the pathophysiology of osteoarthritis. *Nat Rev Rheumatol*. 2011;7(1):33–42. doi:10.1038/nrrheum.2010.196
47. De Roover A, Escribano-Núñez A, Monteagudo S, Lories R. Fundamentals of osteoarthritis: inflammatory mediators in osteoarthritis. *Osteoarthritis Cartilage*. 2023;31(10):1303–1311. doi:10.1016/j.joca.2023.06.005
48. Xia T, Zhang M, Lei W, et al. Advances in the role of STAT3 in macrophage polarization. *Front Immunol*. 2023;14:1160719. doi:10.3389/fimmu.2023.1160719
49. Casanova JL, Holland SM, Notarangelo LD. Inborn errors of human JAKs and STATs. *Immunity*. 2012;36(4):515–528. doi:10.1016/j.immuni.2012.03.016
50. Huynh J, Etemadi N, Hollande F, Ernst M, Buchert M. The JAK/STAT3 axis: a comprehensive drug target for solid malignancies. *Semi Cancer Biol*. 2017;45:13–22. doi:10.1016/j.semcancer.2017.06.001
51. Qiu Z, Xu F, Wang Z, et al. Blockade of JAK2 signaling produces immunomodulatory effect to preserve pancreatic homeostasis in severe acute pancreatitis. *Biochem Biophys Rep*. 2021;28:101133. doi:10.1016/j.bbrep.2021.101133
52. Li X, Jiang M, Chen X, Sun W. Etanercept alleviates psoriasis by reducing the Th17/Treg ratio and promoting M2 polarization of macrophages. *Immunity, Inflammation and Disease*. 2022;10(12):e734. doi:10.1002/iid3.734
53. Chen B, Ning K, Sun ML, Zhang XA. Regulation and therapy, the role of JAK2/STAT3 signaling pathway in OA: a systematic review. *CCS*. 2023;21(1):67. doi:10.1186/s12964-023-01094-4
54. Shao LT, Gou Y, Fang JK, et al. The Protective Effects of Parathyroid Hormone (1–34) on Cartilage and Subchondral Bone Through Down-Regulating JAK2/STAT3 and WNT5A/ROR2 in a Collagenase-Induced Osteoarthritis Mouse Model. *Orthopaedic Surg*. 2021;13(5):1662–1672. doi:10.1111/os.13019
55. Wang W, Han X, Zhao T, Zhang X, Qu P, Zhao H. AGT, targeted by miR-149-5p, promotes IL-6-induced inflammatory responses of chondrocytes in osteoarthritis via activating JAK2/STAT3 pathway. *Clin Experiment Rheumatol*. 2020;38(6):1088–1095.
56. Nasi S, So A, Combes C, Daudon M, Busso N. Interleukin-6 and chondrocyte mineralisation act in tandem to promote experimental osteoarthritis. *Ann Rheumatic Dis*. 2016;75(7):1372–1379. doi:10.1136/annrheumdis-2015-207487
57. Katz JN, Arant KR, Loeser RF. Diagnosis and Treatment of Hip and Knee Osteoarthritis: a Review. *JAMA*. 2021;325(6):568–578. doi:10.1001/jama.2020.22171
58. Kraus VB, McDaniel G, Huebner JL, et al. Direct in vivo evidence of activated macrophages in human osteoarthritis. *Osteoarthritis Cartilage*. 2016;24(9):1613–1621. doi:10.1016/j.joca.2016.04.010
59. Daghestani HN, Pieper CF, Kraus VB. Soluble macrophage biomarkers indicate inflammatory phenotypes in patients with knee osteoarthritis. *ArthritisRheumatol*. 2015;67(4):956–965. doi:10.1002/art.39006
60. Quicke JG, Conaghan PG, Corp N, Peat G. Osteoarthritis year in review 2021: epidemiology & therapy. *Osteoarthritis Cartilage*. 2022;30(2):196–206. doi:10.1016/j.joca.2021.10.003
61. Su S, Tian R, Jiao Y, et al. Ubiquitination and deubiquitination: implications for the pathogenesis and treatment of osteoarthritis. *J Orthop Transl*. 2024;49:156–166. doi:10.1016/j.jot.2024.09.011